

**Carrier-density dependence of magnetic and magneto-optical properties of (Ga,Mn)As**T. Komori,<sup>1</sup> T. Ishikawa,<sup>2</sup> T. Kuroda,<sup>1</sup> J. Yoshino,<sup>1</sup> F. Minami,<sup>1</sup> and S. Koshihara<sup>1,2,3</sup><sup>1</sup>*Department of Physics, Tokyo Institute of Technology, O-okayama 2-12-1, Meguro-ku, Tokyo 152-8550, Japan*<sup>2</sup>*Department of Materials Science, Tokyo Institute of Technology, O-okayama 2-12-1, Meguro-ku, Tokyo 152-8550, Japan*<sup>3</sup>*Kanagawa Academy of Science and Technology, KSP East Building 301, Sakado 3-2-1, Takatu-ku, Kawasaki-shi, Kanagawa 213-0012, Japan*

(Received 18 June 2002; revised manuscript received 2 December 2002; published 17 March 2003)

We studied the magnetic properties and the magnetic circular dichroism (MCD) of (Ga,Mn)As films with two kinds of the hole-carrier density though keeping a constant value in the Mn concentration grown by the molecular beam epitaxy method. To control the carrier density in (Ga,Mn)As, we utilized Sn atoms, which compensate the hole carriers intrinsically doped due to substitution of Mn<sup>2+</sup> atoms for Ga. The magnitude and the spectral shape of the MCD and the magnetic order have shown remarkable dependence on the hole-carrier density. The observed MCD and normal absorption spectral changes depending on the hole-carrier density can be explained by the model proposed by Szczytko *et al.* which includes the effects of the disorder and the change in the Fermi energy level.

DOI: 10.1103/PhysRevB.67.115203

PACS number(s): 75.50.Pp, 75.50.Dd, 78.20.Ls

**I. INTRODUCTION**

III-V- based diluted magnetic semiconductor (DMSs), such as (Ga<sub>1-x</sub>Mn<sub>x</sub>)As and (In<sub>1-x</sub>Mn<sub>x</sub>)As, are attracting attention for the ferromagnetic order of Mn atoms.<sup>1-5</sup> It has been reported that the magnetic property, especially the Curie temperature  $T_c$ , strongly depends on the Mn concentration in (Ga<sub>1-x</sub>Mn<sub>x</sub>)As thin films. In the range of  $x < 0.05$ ,  $T_c$  rises up to 110 K as the value of  $x$  increases.<sup>2,6</sup> In addition, by virtue of the coexistence of a ferromagnetic order with rather high  $T_c$  and the nature of the semiconductor, possible applications, such as in magnetotransport and magneto-optical devices, have also been discussed.<sup>7-12</sup>

In III-V-based DMS materials, hole carriers are generated by the doping of Mn<sup>2+</sup> magnetic ions, which act as acceptors in GaAs and InAs. Thus it is logical to consider that the exchange interaction between the localized  $d$  electrons of Mn<sup>2+</sup> ions and the itinerant hole carriers ( $p$ - $d$  exchange interaction) is the possible origin of the ferromagnetic order.<sup>2</sup> To confirm this model and to clarify the microscopic exchange mechanisms, various experimental and theoretical studies have been conducted.<sup>2,13,14</sup> In (In,Mn)As grown at low temperature, the disappearance of the ferromagnetic order in  $n$ -type samples was confirmed.<sup>15</sup> The hole-carrier density dependence of  $T_c$  in (Ga,Mn)As was also reported.<sup>16</sup> In addition, the temperature and magnetic-field dependence of a magnetic circular dichroism (MCD) in (Ga,Mn)As was reported.<sup>17</sup>

In previous studies, the control of the type (electrons or holes) and/or density of carriers was basically achieved as a result of the change in the degree of compensation of Mn acceptors by deep donors, such as As antisites induced by excess As incorporation.<sup>16</sup> The development of the method for controlling the carrier density, i.e., the hole-carrier density, independent of the Mn concentration  $x$ , is considered to be essential not only for elucidating the role of hole carriers in magnetic properties in this class of materials but also for obtaining basic information to achieve the device application.

Quite recently, the growth of a (Ga<sub>1-x</sub>Mn<sub>x</sub>)As ( $x = 0.013$ ) sample doped with Sn atoms, and its magnetotransport property, was reported.<sup>18</sup> In this literature, it was confirmed that Sn atoms act as a hole compensators as a result of a systematic change in the Sn vapor pressure under the same growth condition. In addition, a change in the magnetotransport property, accompanied by the carrier density controlled by Sn doping, was also reported. In the present study, we report on the experimental results of magnetic properties and the MCD in (Ga<sub>1-x</sub>Mn<sub>x</sub>)As ( $x = 0.02$ ) thin films, which have the two kinds of hole-carrier densities, without changing the value of  $x$  obtained by the same method of Sn atom doping.

The study of optomagnetic properties in DMSs is considered to be of key importance for clarifying the electronic structure, as discussed in II-VI compound-based DMSs,<sup>19-21</sup> as well as for designing device applications such as thin-film magneto-optical isolators.<sup>22</sup> Results reported in Sec. II indicate that the magnitude and the spectral shape of the MCD show a remarkable dependence on the hole-carrier density, strongly correlating with the magnetic order of Mn ions. We tentatively explain the MCD spectra by the theoretical model developed by Szczytko *et al.*,<sup>23</sup> which includes the effects of the change in the Fermi energy level and the disorder caused by the Mn substitution, Sn doping, and low-temperature growth of thin films. These results seem to support the idea that the exchange interaction among localized  $d$  electrons on Mn<sup>2+</sup> atoms and the itinerant hole in the valence band that has an electronic structure similar to that of GaAs rule the magnetic and optomagnetic properties in (Ga<sub>1-x</sub>Mn<sub>x</sub>)As ( $x = 0.02$ ).

**II. EXPERIMENTS AND SAMPLES**

In order to study the MCD spectra and the magnetic properties of (Ga<sub>1-x</sub>Mn<sub>x</sub>)As, we grew 200-nm (Ga<sub>0.8</sub>Al<sub>0.2</sub>)As and (Ga<sub>1-x</sub>Mn<sub>x</sub>)As layers with a thickness of 0.7 or 1.0  $\mu\text{m}$  on a GaAs (001) substrate by the molecular-beam epitaxy method, as shown in the inset of Fig. 1. To obtain

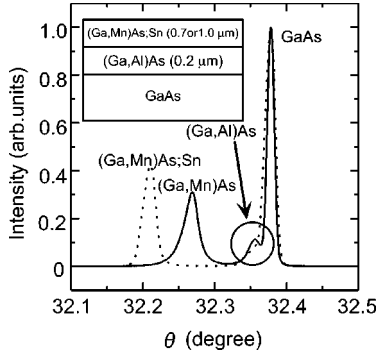


FIG. 1. X-ray- diffraction patterns for No. 1 (Ga,Mn)As (solid line) and No. 2 (Ga,Mn)As;Sn (dotted line). Inset shows the schematic structure of the thin film sample.

( $\text{Ga}_{1-x}\text{Mn}_x$ )As ( $x=0.02$ ) samples [hereafter abbreviated as (Ga,Mn)As] with different carrier densities while keeping the Mn concentration  $x$  at a constant value, we utilized the doping of Sn atoms, which act as a donor.<sup>18</sup> Three types of (Ga,Mn)As with different hole-carrier densities ( $9.3 \times 10^{19}$ ,  $8.8 \times 10^{19}$ , and  $2.2 \times 10^{18} \text{ cm}^{-3}$ ) were prepared by this method. Without the doping of Sn atoms, we can always obtain a ferromagnetic sample with a hole density between  $8.8 \times 10^{19}$  and  $1.2 \times 10^{20} \text{ cm}^{-3}$  under the same growth condition. Therefore the observed decrease in hole density in sample No. 2 can be attributed to the carrier compensation by Sn doping. Hereafter, the ( $\text{Ga}_{1-x}\text{Mn}_x$ )As ( $x=0.02$ ) sample doped with Sn atoms is abbreviated as (Ga,Mn)As;Sn. Samples utilized for the present study as typical examples are listed in Table I. The hole-carrier densities indicated in Table I were estimated by the Hall effect measurement at room temperature under a van der Pauw configuration. The notation of low-temperature(LT)-GaAs in this table represents the GaAs thin films grown at low temperature ( $300 \pm 10^\circ \text{C}$ ) on a GaAs substrate, which is the same temperature utilized for the growth of (Ga,Mn)As and (Ga,Mn)As;Sn layers.

We used the data of x-ray-diffraction measurements to estimate the Mn concentration of thin films, and to check whether Mn(Sn) atoms are uniformly doped as a mixed crystal (Ga,Mn)As(;Sn). Figure 1 shows typical x-ray-diffraction patterns of the samples No. 1 (Ga,Mn)As (solid line) and No. 2 (Ga,Mn)As;Sn (dotted line). A large peak located around  $32.38^\circ$  in Fig. 1 can be assigned to the (004) peak of the GaAs substrate, and the left-hand-side small peak (solid line) and shoulder (dotted line) of this peak are due to the ( $\text{Ga}_{0.8}\text{Al}_{0.2}$ )As [hereafter denoted as the (Ga,Al)As] layer.

TABLE I. Sample list.

	Composition	Mn concentration	Hole carrier density	Layer thickness
No. 1	(Ga,Mn)As	2.1%	$8.8 \times 10^{19} \text{ cm}^{-3}$	$1.0 \mu\text{m}$
No. 2	(Ga,Mn)As;Sn	2.0 %	$2.2 \times 10^{18} \text{ cm}^{-3}$	$1.0 \mu\text{m}$
No. 3	LT-GaAs	-	-	$1.0 \mu\text{m}$
No. 4	(Ga,Mn)As	1.7%	$9.3 \times 10^{19} \text{ cm}^{-3}$	$0.7 \mu\text{m}$

The two peaks of the solid line ( $\sim 32.28^\circ$ ) and the dotted line ( $\sim 32.21^\circ$ ) can be attributed to the diffraction from (Ga,Mn)As and (Ga,Mn)As doped with Sn atoms. The concentration of Mn can be estimated based on the diffraction angle of this peak. In the case of the (Ga,Mn)As;Sn sample, the effect of the lattice expansion due to Sn doping was estimated utilizing the data of the Sn vapor-pressure dependence of a GaAs lattice constant doped with Sn atoms.<sup>24</sup> In addition, the observed widths of two peaks assigned to (Ga,Mn)As and (Ga,Mn)As;Sn are almost the same as that of the GaAs (004) diffraction peak. This result suggests that the structural disorder in (Ga,Mn)As and (Ga,Mn)As;Sn samples induced by Mn and/or Sn doping is not so large as to seriously broaden the x-ray-diffraction peaks.

For the MCD measurement, self-standing thin films were prepared by subtracting the GaAs substrate using the etching technique. A (Ga,Al)As layer of 200-nm thickness grown on the GaAs substrate blocked the progress of the etching process (see the inset of Fig. 1). The MCD spectra were measured on the basis of the difference in absorption for right ( $\sigma^+$ ) and left ( $\sigma^-$ ) circularly polarized light. The magnetic field was set parallel to the direction of the light propagation (Faraday configuration). The temperature dependence of the magnetization (denoted as the  $M$ - $T$  curve) and the magnetic-field dependence of the magnetization ( $M$ - $H$  curve) were observed using a commercially available superconducting quantum interference device(SQUID) magnetometer, with the magnetic field set normal to the sample surface.

### III. RESULTS AND DISCUSSION

#### A. Experimental results of magnetic property and MCD measurement

In Fig. 2, the magnetic properties of two samples [No. 1 (Ga,Mn)As and No. 2 (Ga,Mn)As;Sn] are plotted. Figure 2(a) indicates the  $M$ - $T$  curves in the magnetic field of 0.2 T. Based on this plot, the Curie temperature of No. 1 (Ga,Mn)As (square plots) was estimated to be 60 K. On the other hand, for No. 2 (Ga,Mn)As;Sn, the ferromagnetic order was not observed, and the sample showed paramagnetic behavior, even if the sample was cooled down to 5 K [see triangular plots in Fig. 2(a)]. In addition, the observed  $M$ - $H$  curve of sample No. 1 (squares) showed a hysteresis loop with a coercive field of 0.01 T [see the inset of Fig. 2(b)], and the magnetization was saturated at  $\pm 0.15$  T. In contrast, that for sample No. 2 did not show a hysteresis loop. The magnetic properties of sample No. 1 and No. 2 are quite different even though the Mn concentrations of both samples are about the same value (2.1% and 2.0%, respectively). This result strongly supports the previously discussed idea that hole carriers are a key factor in the ferromagnetic interaction between Mn spins.<sup>2</sup>

As a first step in an investigation into the relation between the MCD spectrum and the magnetic property, we measured the temperature and magnetic-field dependences of the MCD signal observed at 1.73 eV. Figure 3 shows the results for sample No. 4 (Ga,Mn)As, which has similar physical properties to sample No. 1. The obtained results indicate a parallel relation between the magnetization and the MCD signal at

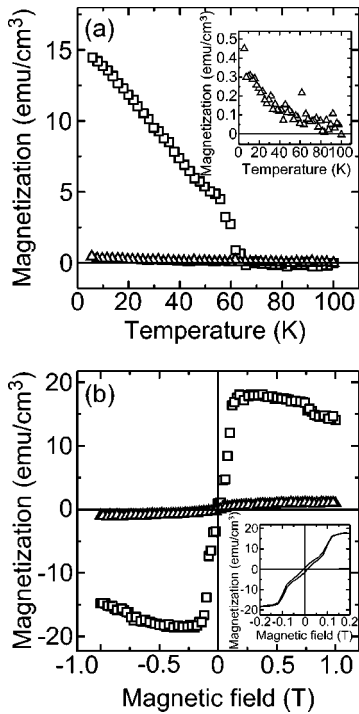


FIG. 2. Magnetic properties of No. 1 (Ga,Mn)As (square plots) and No. 2 (Ga,Mn)As;Sn (triangular plots). (a)  $M$ - $T$  curve at a magnetic field of 0.2 T; the inset shows the expansion of the  $M$ - $T$  curve of No. 2. (b)  $M$ - $H$  curve at a temperature of 5.0 K; inset shows the expansion of the  $M$ - $H$  curve of No. 1 (Ga,Mn)As.

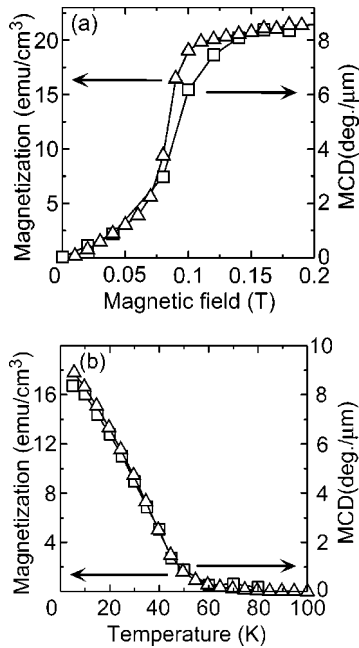


FIG. 3. (a) Magnetic-field dependence of the MCD (1.73 eV) (open squares) and magnetization (open triangulars) of sample No. 4 (Ga,Mn)As at a temperature of 5.0 K. (b) Temperature dependence of the MCD (1.73 eV) (open squares) and the magnetization (open triangulars) of the sample at a magnetic field of 0.2 T.

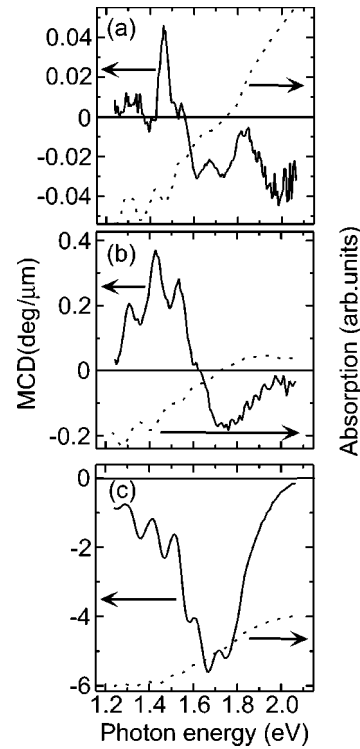


FIG. 4. MCD (solid lines) and absorption (dotted lines) spectra of (a) No. 3 LT-GaAs, (b) No. 2 (Ga,Mn)As;Sn, and (c) No. 1 (Ga,Mn)As at 5.0 K and magnetic field at 1.0 and 0 T for the MCD and the absorption spectra, respectively.

1.73 eV for this sample. Therefore, we can safely conclude that the observed MCD signal has a close correlation with the ordering of Mn spins. In addition, a similar parallel behavior was confirmed for sample No. 2.

The MCD spectra of three samples, Nos. 3, 2, and 1, observed at 5 K in the magnetic field of 1.0 T are plotted in Figs. 4(a), 4(b), and 4(c), respectively (solid lines), with absorption spectra (dotted lines). These MCD spectra are indicated in units of the Faraday rotation angle for a probe light path length of 1  $\mu\text{m}$ . The periodically oscillating structure observed in a photon energy region lower than 1.7 eV of absorption and MCD spectra can be attributed to the interference effect of the reflected monitor light in the thin film samples. The MCD spectrum of sample No. 3 LT-GaAs [see Fig. 4(a)] showed a maximum around 1.45 eV, and decreased its magnitude to zero around 1.52 eV (hereafter referred to as the zero crossing point energy,  $E_{zero}$ ). The observed MCD spectrum for this sample corresponds to the previously reported one, whose origin was attributed to the Zeeman splitting of the electronic states located around the band edge of GaAs.<sup>25</sup>

The spectral shapes of the MCD of samples No. 2 and No. 3 have common characteristics in spite of the discrepancy in the magnitude [see Figs. 4(a) and 4(b)]. The MCD spectrum of sample No. 2 [Fig. 4(b)] also shows  $E_{zero}$  at 1.62 eV, and changes sign from positive to negative like sample No. 3 [Fig. 4(a)], except for a discrepancy in the  $E_{zero}$  value (about 100 meV higher than that for No. 3). In contrast, the MCD spectrum of sample No. 1 ((Ga,Mn)As with high hole den-

sity) is quite different from those of No. 2 and No. 3 in both the spectral shape and magnitude. It is worthy of note that the MCD spectrum of No. 1 has a negative sign and a very broad structure that does not show the zero crossing point within the energy range of the present measurement (1.2–2.1 eV). These results clearly indicate that both the magnitude of the MCD and its spectral shape remarkably change according to the hole-carrier density and show the close correlation with magnetic property.

### B. Comparison with theoretically calculated MCD spectra

As is well known, the magneto-optical properties in II-VI-based DMSs can be well explained by the Zeeman splitting effect of the band-edge state based on the exchange interaction between localized  $d$  electrons of  $\text{Mn}^{2+}$  ions and itinerant band electrons ( $s$ ,  $p$ - $d$  exchange interactions).<sup>19–21,26</sup> It is important to determine whether a similar mechanism can explain the MCD spectra in III-V-based DMSs. This subject has a close relation with the fundamental mechanism of magnetic exchange interaction in this class of DMSs. As for the MCD spectrum of  $(\text{Ga}_{1-x}\text{Mn}_x)\text{As}$ , extensive studies have been conducted on its  $x$  and magnetic-field dependences to clarify the electronic origin.<sup>17,25</sup> In the following part of this paper, we show that the obtained hole-carrier density dependence of the MCD spectral shape can be explained by the method proposed by Szczytko *et al.*<sup>23</sup>

In  $(\text{Ga}, \text{Mn})\text{As}$  thin films, the effects of disorder caused by doping of Mn and/or Sn impurities and the defects due to the low-temperature growth of the  $(\text{Ga}, \text{Mn})\text{As}$  layer logically become very large. In addition, it should be noted that the change in the Fermi energy level will also be very large because the concentration of the doped Mn acceptors reaches the order of  $10^{19} \text{ cm}^{-3}$ .<sup>27</sup> Quite recently, Szczytko *et al.* developed a method for the calculation of the MCD spectra for  $(\text{Ga}_{1-x}\text{Mn}_x)\text{As}$  based on the optical transition between the band-edge states of pure GaAs modified by the disorder effect and the change in the Fermi energy level.<sup>23</sup> The solid and dashed lines in Fig. 5 show the hole-density ( $n_p$ ) dependence of the calculated MCD and the normal absorption spectra based on this method. The calculated spectra for the hole densities of  $n_p = 1 \times 10^{19}$  and  $1 \times 10^{18} \text{ cm}^{-3}$  are plotted in Figs. 5(a) and 5(b), respectively, as typical examples, and they seem to reproduce well the observed MCD (open squares) and absorption (open triangles) spectra of samples No. 1 [(Ga,Mn)As] [see Fig. 5(a)] and No. 2 [(Ga,Mn)As:Sn] [see Fig. 5(b)]. Nn anomaly of around 1.8 eV in the calculated spectrum in Fig. 5(a) is attributed to Zeeman split of the spin-orbit band. Of course, the calculated spectral shape strongly depends on the various physical parameters, and it should thus be noted that proper values for them corresponding to samples No. 1 and No. 2 (see Table II) have to be utilized for calculation. We consider the used parameter values for the present calculation are reasonable ones as discussed in the following part.

As for the thermodynamic average of the spin value  $\langle S \rangle$  at 1 T, which is necessary for the estimation of the effective values of the band gap  $E'_g$  and the Fermi energy  $F'$  under a

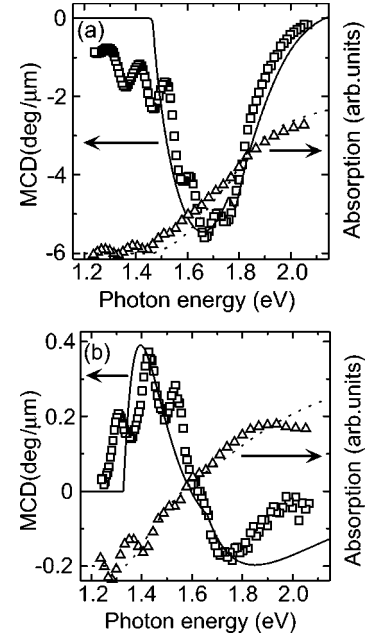


FIG. 5. Hole-carrier density dependence of the observed (square and triangular plots) and calculated (solid and dotted lines) MCD and absorption spectra for (a) No. 1  $(\text{Ga}, \text{Mn})\text{As}$  and (b) No. 2  $(\text{Ga}, \text{Mn})\text{As}:\text{Sn}$ . As for absorption spectra, the results of theoretical calculation for zero magnetic field are indicated.

magnetic field, the values observed for corresponding samples Nos. 1 and 2 (2.5 and 0.14) by a SQUID magnetometer were utilized. The Mn concentration for both cases was commonly set to 2.0% based on the estimate of the lattice constant by x-ray-diffraction method for our samples (see Table I). Following the method of Szczytko *et al.*, we assumed that the values of exchange constants for the conduction ( $s$ - $d$ ) ( $N_0\alpha$ ) and valence ( $p$ - $d$ ) ( $N_0\beta$ ) bands were 0.2 and -1.0 eV, respectively. The band-gap energy  $E_g$  was properly adjusted to 1.43 eV (1.32 eV) for the case shown in Fig. 5(a) [and Fig. 5(b)] to reproduce the experimentally observed MCD spectra of sample No. 1 (No. 2). The utilized value of  $E_g$  was considerably small compared to that of pure GaAs. The observed expansion of the lattice constant (see Fig. 1) and the expected gap energy shrinkage due to the many-body effect in  $(\text{Ga}, \text{Mn})\text{As}$  seem to be consistent with the rather low estimated  $E_g$ . Other band parameters (such as the effective mass) were set to the same values as those of pure GaAs.<sup>23</sup>

TABLE II. Parameter list utilized for fitting shown in Fig. 6.

	No. 1 $(\text{Ga}, \text{Mn})\text{As}$	No. 2 $(\text{Ga}, \text{Mn})\text{As}:\text{Sn}$
$n_p$	$1 \times 10^{19} \text{ cm}^{-3}$	$1 \times 10^{18} \text{ cm}^{-3}$
$E_g$	1.43 eV	1.32 eV
' $a$ '	65 Å	15 Å
$\langle S \rangle$	2.5	0.14
Mn concentration	2.0 %	2.0 %
$N_0\alpha$	0.2	0.2
$N_0\beta$	-1.0	-1.0



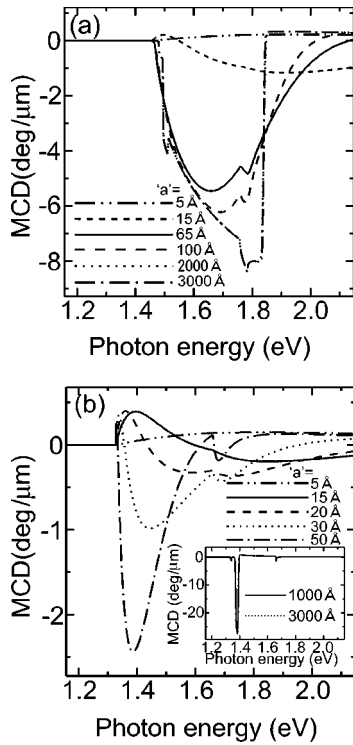


FIG. 6. Calculated MCD spectra for various  $a$  values. (a) shows the MCD spectra of  $n_p = 1 \times 10^{19} \text{ cm}^{-3}$ . (b) shows the spectra corresponding to  $n_p = 1 \times 10^{18} \text{ cm}^{-3}$ .

The carrier density  $n_p$  values utilized for the MCD calculation [ $1 \times 10^{19} \text{ cm}^{-3}$  for Fig. 5(a) and  $1 \times 10^{18} \text{ cm}^{-3}$  for Fig. 5(b)] were much smaller than those estimated at room temperature (see Table I). It has been previously reported that  $n_p$  shows a strong dependence on the sample temperature.<sup>18</sup> As for our samples, i.e., ferromagnetic (Ga,Mn)As thin films doped with Sn atoms, the estimation of  $n_p$  value based on the residual magnetization-temperature characteristics demonstrated that the  $n_p$  at room temperature was about ten times larger than that at 60 K.<sup>18</sup> Based on this previous work, the  $n_p$  values utilized here for the calculation are considered to be reasonable ones. Of course, due to the large anomalous Hall effect in (Ga,Mn)As, a measurement under a very high magnetic field over 20 T is necessary for a more correct and direct estimation of the  $n_p$  value at low temperature by the normal Hall effect.<sup>6</sup>

The calculated results of normal absorption and the MCD shown in Figs. 5(a) and 5(b) (dotted and solid lines) were obtained by setting  $a = 65$ , and  $15 \text{ \AA}$ , respectively. The value ' $a$ ' stands for the degree of the expanse of the electric wave function. It corresponds to the  $\sigma^{-1}$  value in Ref. 23, and can be regarded as the indicator of the degree of the disorder (as the disorder becomes larger, the value of  $a$  decreases). Fig-

ures 6(a) and 6(b) show the calculated MCD spectra for various  $a$  values with  $n_p = 1 \times 10^{19}$  and  $n_p = 1 \times 10^{18} \text{ cm}^{-3}$ , respectively. Based on these figures, the utilized  $a$  values seem to be proper ones for the consistent fitting of the experimental results of MCD and normal absorption spectra shown in Figs. 5(a) and 5(b).

The  $a$  value estimated for sample No. 2 was much smaller than that for sample No. 1. We now tentatively assigned the origin of the observed decrease in the  $a$  value to the disorder induced by additional Sn doping. Of course, it is a problem that the compensated hole density is not so large ( $\sim 9 \times 10^{19} \text{ cm}^{-3}$ ) though a large amount of Sn atoms seem to be doped in the sample, as reflected in the apparent decrease of the  $a$  value. This result may suggest that only a part of Sn atoms are active as electron donors for hole compensation. The nature of Sn atoms doped in GaAs is not clear at the present stage, especially under the condition of high density doping. Therefore, a detailed analysis of the behavior of doped Sn atoms in (Ga,Mn)As is left as a future problem.

Based on these considerations, we conclude that the observed results of MCD and normal absorption measurement can be explained by the theoretical model of Szczytko *et al.* In other words, the MCD and normal absorption spectra and their dependences on the hole-carrier density observed for (Ga,Mn)As and (Ga,Mn)As:Sn samples can be basically explained by the spin-splitting effect in the valence band, taking into account the change in the Fermi energy level and the disorder effect. Based on our calculation, the spin-splitting value and the Fermi energy level from the top of the valence band on sample No. 1 have been estimated to be 50 and 54 meV, respectively.

#### IV. SUMMARY

We found that the magnetic property and the spectral shape of the MCD show remarkable differences between (Ga,Mn)As samples with two different hole-carrier densities, both of which have the same Mn concentration. We also found that the observed MCD and normal absorption spectra of (Ga,Mn)As, and their dependence on the hole density, can be consistently explained by the model proposed by Szczytko *et al.* utilizing reasonable values for various physical parameters, including the effects of the change in the Fermi energy level and the disorder. In other words, the observed results support the idea that the origin of the MCD in (Ga,Mn)As is the spin-splitting effect in the electronic band structure, which is analogous to that of GaAs.

#### ACKNOWLEDGMENTS

This work was partially supported by NEDO and a Grant-in-aid for Scientific Research from Ministry of Education, Culture, Sports, Science and Technology. We thank Y. Satoh for his help in the MBE sample growth.

<sup>1</sup>H. Ohno, A. Shen, F. Matsukura, A. Oiwa, A. Endo, S. Katsumoto, and Y. Iye, *Appl. Phys. Lett.* **69**, 363 (1996).

<sup>2</sup>F. Matsukura, H. Ohno, A. Shen, and Y. Sugawara, *Phys. Rev. B* **57**, R2037 (1998).

<sup>3</sup>H. Ohno, *Science* **281**, 951 (1998).

<sup>4</sup>H. Ohno, *J. Magn. Magn. Mater.* **200**, 110 (1999).

<sup>5</sup>H. Ohno, H. Munekata, T. Penney, S. von Molnár, and L.L. Chang, *Phys. Rev. Lett.* **68**, 2664 (1992).

- <sup>6</sup>H. Ohno, F. Matsukura, T. Omiya, and N. Akiba, *J. Appl. Phys.* **85**, 4277 (1999).
- <sup>7</sup>T. Hayashi, H. Shimada, H. Shimizu, and M. Tanaka, *J. Cryst. Growth* **201/202**, 689 (1999).
- <sup>8</sup>D. Chiba, N. Akiba, F. Matsukura, Y. Ohno, and H. Ohno, *Physica E* **10**, 278 (2001).
- <sup>9</sup>N. Akiba, D. Chiba, K. Nakata, F. Matsukura, Y. Ohno, and H. Ohno, *J. Appl. Phys.* **87**, 6436 (2000).
- <sup>10</sup>S. Koshihara, A. Oiwa, M. Hirasawa, S. Katsumoto, Y. Iye, C. Urano, H. Takagi, and H. Munekata, *Phys. Rev. Lett.* **78**, 4617 (1997).
- <sup>11</sup>A. Oiwa, Y. Mitsumori, R. Moriya, T. Ślupinski, and H. Munekata, *Phys. Rev. Lett.* **88**, 137202 (2002).
- <sup>12</sup>Y. Ohno, D.K. Young, B. Beschoten, F. Matsukura, H. Ohno, and D.D. Awschalom, *Nature (London)* **402**, 790 (1999).
- <sup>13</sup>J. Okabayashi, A. Kimura, O. Rader, T. Mizokawa, A. Fujimori, T. Hayashi, and M. Tanaka, *Phys. Rev. B* **58**, R4211 (1998).
- <sup>14</sup>T. Ogawa, M. Shirai, N. Suzuki, and I. Kitagawa, *J. Magn. Magn. Mater.* **196/197**, 428 (1999).
- <sup>15</sup>S. von Molnár, H. Munekata, H. Ohno, and L.L. Chang, *J. Magn. Magn. Mater.* **93**, 356 (1991).
- <sup>16</sup>M. Tanaka, *J. Cryst. Growth* **201/202**, 660 (1999).
- <sup>17</sup>B. Beschoten, P.A. Crowell, I. Malajovich, D.D. Awschalom, F. Matsukura, A. Shen, and H. Ohno, *Phys. Rev. Lett.* **83**, 3073 (1999).
- <sup>18</sup>Y. Satoh, D. Okazawa, A. Nagashima, and J. Yoshino, *Physica E* **10**, 196 (2001).
- <sup>19</sup>*Diluted Magnetic Semiconductors, Semiconductors and Semimetals*, edited by J. K. Furdyna and J. Kossut (Academic, Boston, 1988), vol. 25.
- <sup>20</sup>J.K. Furdyna, *J. Appl. Phys.* **64**, R29 (1988).
- <sup>21</sup>W. Mac, Nguyen The Khoi, A. Twardowski, and J.A. Gaj, *Phys. Rev. Lett.* **71**, 2327 (1993).
- <sup>22</sup>T. Kuroiwa, T. Yasuda, F. Matsukura, A. Shen, Y. Ohno, Y. Segawa, and H. Ohno, *Electron. Lett.* **34**, 190 (1998).
- <sup>23</sup>J. Szczytko, W. Bardyszewski, and A. Twardowski, *Phys. Rev. B* **64**, 075306 (2001).
- <sup>24</sup>Y. Satoh, N. Inoue, Y. Nishikawa, and J. Yoshino, in *Proceeding of Third Symposium on the Physics and Application of Spin-Related Phenomena in Semiconductors* (Sendai, Japan, 1997), p. 23.
- <sup>25</sup>K. Ando, T. Hayashi, M. Tanaka, and A. Twardowski, *J. Appl. Phys.* **83**, 6548 (1998).
- <sup>26</sup>D.U. Bartholomew, J.K. Furdyna, and A.K. Ramdas, *Phys. Rev. B* **34**, 6943 (1986).
- <sup>27</sup>J. Szczytko, W. Mac, A. Twardowski, F. Matsukura, and H. Ohno, *Phys. Rev. B* **59**, 12 935 (1999).